DOI: 10.1002/masy.200950508

Ferroelectric Poly(vinylidene fluoride-trifluoroethylene-chlorotrifluoroethylene)s: Effect of Molecular Weight on Dielectric Property

Chuanqi Zhao,[1,2] *Maotian Guo,*[2] *Yingying Lu,*[1] *Qing Wang**[1]

Summary: A series of ferroelectric poly(vinylidene fluoride-trifluoroethylene-chlorotrifluoroethylene), P(VDF-TrFE-CTFE), have been synthesized by a two-step approach. The first step is copolymerization of VDF and CTFE via solution or suspension methods to produce P(VDF-CTFE) copolymers with different molecular weights. The second step is partial de-chlorination to convert copolymers into P(VDF-TrFE-CTFE) terpolymers with precisely controlled compositions. The effect of molecular weight, molecular weight distribution and uniaxially stretching on the dielectric properties has been investigated over a broad range of temperature and frequency. The X-ray diffraction patterns and DSC curves demonstrate the coexistence of the multiple phases in the terpolymers. The dielectric spectra depict the local relaxation processes and relaxor ferroelectric behavior on the basis of the dielectric loss tangent as a function of temperature.

Keywords: dielectrics; ferroelectric polymers; poly(vinylidene fluoride-trifluoroethylene-chlorotrifluoroethylene); polymer molecular weight

Introduction

Ferroelectric polymers have stimulated extensive research interest in recent years due to their great potentials in advanced applications such as actuators, capacitors, memories, transducers and sensors.[1–5] Compared to conventional inorganic ceramics, polymeric dielectric materials possess many inherent advantages including light weight, flexibility, large-scale processability, high electrical breakdown strength, and excellent reliability. Poly(vinylidene fluoride) (PVDF) based homo- and co-polymers are well-known and extensively studied ferroelectric materials.[6] Their interesting electronic properties originate from the spontaneous alignment of the C-F dipoles in the crystalline phases of the polymers. Depending on the processing conditions, the polymer chains in PVDF can be packed into various crystal lattices, resulting in different crystalline phases including non-polar α phase with *trans-gauche* conformation, polar β phase with *all-trans* zigzag chain conformation, and polar γ phase with *trans-trans-trans-gauche* conformation.[7] The switches between non-polar and polar phases can be induced by electric field poling, fast heating or cooling, high pressure, and mechanical stretching.[8] During the phase transition, dipole moments and lattice parameters are greatly modified, leading to significant changes of dielectric constants and interesting electromechanical responses.

The energy barriers of the phase transition are different for PVDF homo- and copolymers, which is closely related to the chain structures.[9] PVDF shows a relatively low dielectric constant at about 10 at room temperature due to its high crystallinity and

---

[1] Department of Materials Science and Engineering, The Pennsylvania State University, University Park, Pennsylvania, 16802 USA
Fax:(+1)814 8652917; E-mail: wang@matse.psu.edu
[2] School of Physics and Engineering, Zhengzhou University, Zhengzhou, 450052 P. R. China

large crystal lattice size. As a result of its high energy barrier of the phase transition, the ferroelectric-paraelectric (F-P) phase transition (*i.e.* Curie transition) in PVDF can not be observed below the melting point. By introducing the structural defects, such as trifluoroethylene (TrFE) units, into the polymer chain, the extra fluorine atoms in TrFE prevents the polymer chain adopting the *trans-gauche* conformation. As a result, the copolymer P(VDF-TrFE) forms ferroelectric β phase with *all-trans* chain conformation and a polar crystal lattice. The lowest Curie transition temperature for P(VDF-TrFE) copolymer appears at $\sim$60 °C with 45 mol% TrFE in the copolymer.[10–14] The introduction of the third bulky monomer, such as chlorotrifluoroethylene (CTFE), 1,1-chlorofluoroethylene (CFE), hexafluoropropylene (HFP), as crystalline defects into P(VDF-TrFE), further decreases the energy barrier of the phase transition. The resulting terpolymers exhibit high dielectric constants and large electrostrictive responses at room temperature.[15–17] It has been reported that electron or gamma irradiation can also introduce structural defects into the ferroelectric P(VDF-TrFE) copolymers, which reduces or even eliminates the transition barrier between the polar-nonpolar phase transitions.[18] Consequently, the phase transition for irradiated copolymer P(VDF-TrFE) and the terpolymers containing bulky third monomers can be efficiently induced by an applied electric field with very little hysteresis at room temperature.

In our previous studies, it has been found that the molecular weight of P(VDF-CTFE) copolymers and the chemical composition of the P(VDF-TrFE-CTFE) terpolymers have a strong impact on the phase transition, the dielectric properties and the electric breakdown strength.[19–21] Herein, we report the synthesis and processing of the P(VDF-TrFE-CTFE) terpolymers with varied molecular weights. The dependence of the polarization dynamics, the dielectric properties, and the electric energy densities of the polymers on molecular weight and molecular weight distribution has been investigated.

Experimental Part

All solvents and reagents were purchased from VWR and used as received unless otherwise noted. Ethyl hydroxyethyl cellulose was used as received from Polymer Lab Inc. Tetrahydrofuran (THF) was distilled from sodium/benzophenone ketyl under Argon protection. Vinylidene fluoride and chlorotrifluoroethylene were purchased from SynQuest Laboratory Inc. and purified by the freeze-thaw process prior to use.

The copolymerization procedures of VDF and CTFE by solution and suspension methods were performed according to the references.[22–23] The chain transfer agent, diethyl carbonate, was added into suspension polymerization to control the molecular weight and molecular weight distribution.[19] A typical suspension polymerization procedure is as followed. To a 300-mL stainless steel autoclave equipped with a mechanical stirrer, hydrogen peroxide (0.27 g, 2.1 mmol), ethyl hydroxyethyl cellulose (0.16 g), diethyl carbonate (0.05 mL, 0.4 mmol) and degassed distilled water (150 mL) were added. The reactor was degassed by repeated freeze-thaw cycles and then cooled by liquid nitrogen. The reaction mixture was heated at 110 °C for 4 hrs after VDF (33 g) and CTFE (15 g) were condensed and transferred into the reactor. P(VDF-CTFE) (20 g) was obtained after filtration and purification by washing with methanol and distilled water and drying in vacuo at 60 °C for 24 hrs. The solution polymerization was carried out according to a similar procedure to the suspension method except using acetonitrile as solvent, dibenzyl peroxide as initiator and that the reaction temperature is 80 °C and polymerization time is 6 hrs. The subsequent de-chlorination of P(VDF-CTFE) to prepare P(VDF-TrFE-CTFE) was performed following a procedure described elsewhere.[21]

Polymer films with a thickness around 20 μm were prepared by solution casting from DMF solution onto the glass slides modified by *n*-octyltrichlorosilane. The polymer solution was filtered through 0.45 μm poly(tetrafluoroethylene) filters before casting.

The films were dried at 60 °C overnight followed by heating at the same temperature under vacuum for 24 hrs. Free-standing films were created by peeling off carefully. The prepared polymer films were uniform, colorless and transparent. Gold electrodes with a thickness of ~60 nm were sputtered onto the films for electrical characterization. ^{1}H and ^{19}F NMR spectra were recorded on a Bruker AM-300 spectrometer instrument. Gel permeation chromatograph (GPC) was performed using DMF as the mobile phase with a Viscotek TDA 302 triple detector system. The thermal transition data were obtained using a TA Q100 instrument at a heating rate of 10 °C/min. Wide-angle x-ray diffraction (WAXD) measurements were conducted using a Scintag Cu-K$_\alpha$ diffractometer with an X-ray wavelength of 1.54 Å. FTIR spectra were recorded on a Varian Digilab FTS-800 FTIR spectrometer. Dielectric properties were acquired using an Agilent LCR meter (E4980A). Electrical breakdown was performed using a Trek Model 30/20 ± 30 KV high voltage amplifier system in Galden HT fluid. Polarization versus electric field measurement were carried out using a Sawyer-Tower circuit at 10 Hz with bipolar field.

Results and Discussion

Synthesis

The synthetic approach involves the copolymerization of VDF and CTFE and the following de-chlorination reaction. P(VDF-CTFE)s were prepared via solution and suspension methods, respectively. In solution polymerization, acetonitrile was used as solvent and the free radial initiator was benzyl peroxide. The copolymers prepared via solution method are of relatively low molecular weight (~40 kDa) due to high rate of termination reaction in a homogeneous polymerization system. While for the suspension polymerization with distilled water as solvent, hydrogen peroxide as initiator and ethyl hydroxyethyl cellulose as surfactant, higher molecular weight copolymers (~240 kDa) were obtained because of the heterogeneous condition and the resulting low rate of termination reaction. In order to achieve a relatively narrow polydispersity and to prevent the formation of ultra-high molecular weight polymers, chain transfer agent, such as diethyl carbonate, was added to control the molecular weight and molecular weight distribution in the suspension polymerization. Relatively narrow molecular weight distribution could also be obtained by decreasing the conversion of monomers in the suspension polymerization. The chemical compositions of P(VDF-CTFE) copolymers are readily controlled by varying the monomer feeding ratios, as VDF and CTFE have similar reactivity ratios in free radical polymerization (*i.e.* r(VDF) = 0.70, r(CTFE) = 0.72). The synthesis of P(VDF-TrFE-CTFE) by de-chlorination reaction was carried out using *n*-tributyltin as an reduction agent in THF. By adjusting the ratio of the reduction agent and CTFE content in P(VDF-CTFE), the quantitative yield of de-chlorination leads to a well-controlled TrFE concentration in the terpolymers.

As shown in Scheme 1, four P(VDF-TrFE-CTFE) terpolymers were prepared in this study. Polymer **I** with relatively low molecular weight was prepared from the solution-polymerized copolymers. Polymers **II** and **III** were synthesized using the suspension-polymerized copolymers that were quenched in different conversions. Polymer **II** was further uniaxially stretched to give polymer **II′**. The detailed molecular weights, polydispersity indexes (PDI), and chemical compositions of the polymers are listed in Table 1. The superimposed Mark-Houwink plots of intrinsic viscosity versus

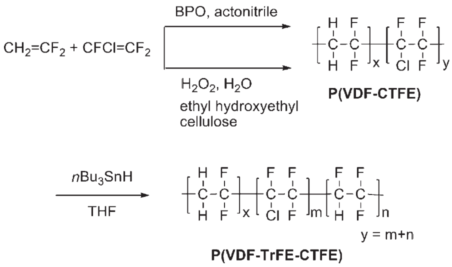

Scheme 1.
Synthesis of P(VDF-TrFE-CTFE).

Table 1.
The chemical composition, molecular weight and molecular weight distribution of the polymers.

Polymer	Composition/ mol% VDF/ TrFE/CTFE	M_n (kDa)	PDI
I	78.8/7.2/14.0	40	1.8
II	78.9/7.1/14.0	240	2.2
III	78.9/7.2/13.9	226	1.7

molecular weight of the polymers indicate that their chain structures are similar without significant differences in branching. The ^{1}H and ^{19}F NMR spectra also confirm the similarity of the molecular structures of these polymers.

Crystalline Structure and Thermal Property

As shown in Figure 1, the WAXD patterns of the polymers generally display a prominent peak centered at a 2θ angle of 18° with a broad peak at approximately 39°. The peak at 18° is assigned to the (002, 020) reflection faces of ferroelectric γ phase and the peak at 39° is the characteristics of (002) reflections of non-polar α phase. There are two weak broad peaks around 17° and 20° that represent the (100) and (110) reflections of non-polar α phase respectively. The qualitative degree of crystallinity calculated from the XRD curves decrease from 36.3% to 24.7% as the molecular weight increases.[19] The lower molecular weight is favorable for the crystallization process presumably through the less inter and intra-chain entanglement.[7] The degree of crystallinity of high molecular weight polymer **II** is believed to be much lower than the calculated result, which is evidenced by the broad thermal transition of the melting process and low enthalpy measured by differential scanning calorimeter (DSC). An actual quantitative calculation of the degree of crystallinity could not be performed due to the lack of an appropriate polymer standard. As illustrated in Figure 2, the low molecular weight polymer **I** shows sharp melting and crystalline peaks with high enthalpy, while the high molecular weight polymers **II** and **III** exhibit much broad melting and crystalline peaks with lower enthalpies, indicating the less perfect and smaller crystals in the high molecular weight polymers with broad crystal size distribution. This is consistent with the decreased crystallite size calculated based on the XRD patterns.

The Dielectric Property

As the ferroelectric phenomena and phase transitions mainly occur in the crystal regions of the polymers, the crystallinity modulated by the molecular weight thereby has great influence on the resulting dielectric properties of the polymers, which allows an unique establishment of the molecular weight–dielectric property correlation. The static and dynamic dielectric properties were measured at room temperature under varied frequencies and temperatures. It is shown in Figure 3 that at room temperature, the dielectric permittivity (ε') of polymers **I**, **II** and **III** are 50, 20 and 45 respectively at 1 kHz. The high molecular weight polymers **II** and **III** possess a similar dielectric loss

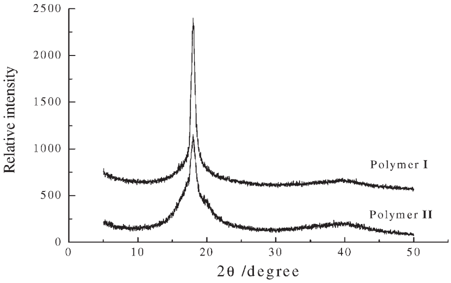

Figure 1.
Wide angle x-ray diffraction patterns of polymers **I** and **II**.

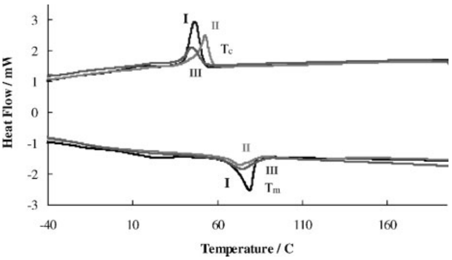

Figure 2.
DSC curves of polymers **I**, **II** and **III** recorded at the second heating and cooling cycle at a rate of 10 °C/min.

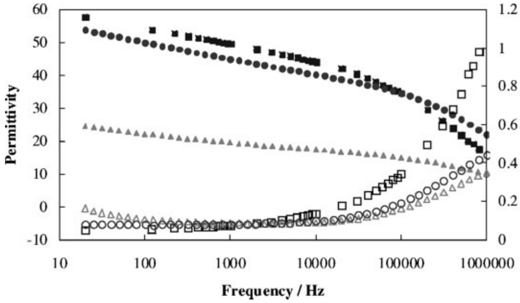

Figure 3.
Permittivity and loss (tan δ) of the polymers as a function of frequency (Hz); ■: permittivity of polymer **I**; □: loss of polymer **I**; ▲: permittivity of polymer **II**; △: loss of polymer **II**; ●: permittivity of polymer **III**; ○: loss of polymer **III**.

(tan δ) in the 20 Hz to 1 MHz range with a flat response of 0.08 between 100 Hz and 10 kHz. Above 10 kHz, tan δ begins to rise rapidly and is related to the dipolar relaxation in the polymers. The low molecular weight polymer **I** shows significantly higher loss than high molecular weight polymers **II** and **III**, which is presumably due to its higher crystallinity and more polar domain phase. Higher dielectric loss at frequencies below 100 Hz has been observed in polymers **II** and **III** compared to that in polymer **I**. This is ascribed to the higher inter- and intra-molecular relaxation times associated with the high molecular weight polymers. With the increase of frequency, the dipolar contribution to permittivity decreases, resulting in a decreased dielectric permittivity.

Due to their semicrystalline nature, PVDF based ferroelectric polymers possess sophisticated relaxation processes including the molecular relaxations in amorphous and crystalline phases as well as the interface. As shown in Figure 4, the dielectric spectra ε' of polymers **I** and **II** as a function of temperature elucidate two strong relaxation processes in the range of -45 to $50\,^{\circ}$C. A low temperature relaxation (denoted as β_r) at $-25\,^{\circ}$C is associated with the dynamic manifestation of the glass transition in the amorphous phase of the polymers. The high-temperature relaxation referred to β_c at $10\,^{\circ}$C is related to the re-orientation dynamics of the crystal domains.[13,24–25] While the nature of the β_c process is still under discussion, it is believed that the primary contribution also comes from the relaxation of chains at the amorphous/crystalline interface, which becomes more convincible for polymer **I** with higher crys-

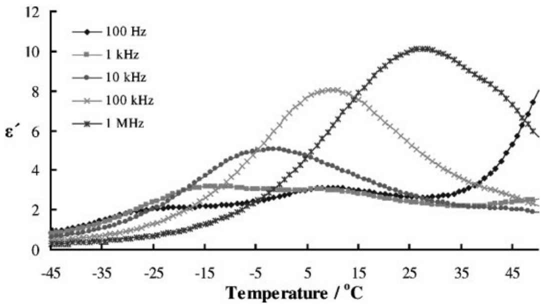

Figure 4.
Dielectric spectra of P(VDF-TrFE-CFE) terpolymers at different frequencies.

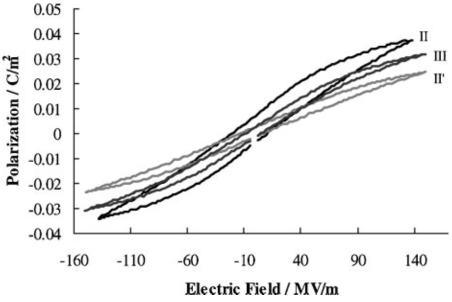

Figure 5.
Polarization hysteresis loop measured at room temperature under 150 MV/m for polymers **II**, **II′** and **III**.

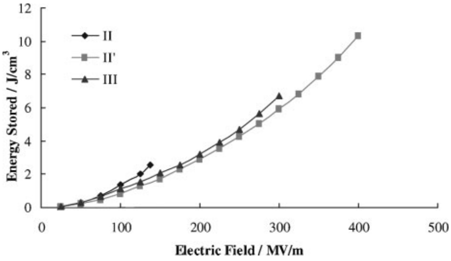

Figure 7.
Stored energy density versus applied electric field for the polymers.

tallinity. Overall, polymer **II** with high molecular weight displays a much broad distribution, which in general reflects heterogeneity at the molecular level: such as the presence of random defects in the crystalline phase originated from the enhanced inter and intra-chain entanglement among the long polymer chains. The broadening with decreasing temperature also suggests that the intermolecular cooperativity increases at lower temperatures due to the reduced fractional free volume and/or chain mobility.[26]

Polarization Responses and Energy Density

As has been revealed in the earlier studies of PVDF and PVDF based copolymers, such as P(VDF-CTFE) and P(VDF-HFP), the polymers can be converted from α to β phases by mechanical stretching, which is a thermodynamically lower energy phase for PVDF and PVDF based copolymers. The polarization-electric field (D-E) hysteresis loop measured from the uniaxially stretched P(VDF-CTFE) (91/9 mol%) films also exhibits a much smaller remnant polarization as compared with that of PVDF.[5,27–28] Figure 5 shows the typical hysteresis loops of the polymers **II**, **II′** and **III** measured at room temperature under 10 Hz and 150 MV/m. Smaller remnant polarization has been demonstrated in the uniaxially stretched polymer film **II′** and the high molecular weight polymer **III** with a narrower molecular weight distribution. Additionally, polymer films **II′** and **III** show much higher electric field strengths, i.e. 400 and 300 MV/m, compared to polymer **II** having a breakdown strength of 138 MV/m. The coercive field (E_c) of polymers **II**, **II′** and **III** is about 12.5, 6.8 and 4.4 MV/m, respectively. The change of the maximum polarization P_s and the ratio between the remnant polarization and maximum polarization (P_r/P_s) as a function of electric field is summarized in Figure 6. Both P_s and P_r/P_s increase as the electric field increases. Polymer **II** shows the highest P_s and P_r/P_s at low electric fields, indicating the early polarization saturation and consequently lower energy density compared with those in polymers **II′** and **III**.

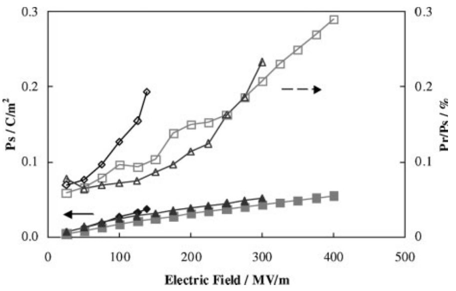

Figure 6.
Maximum polarization (P_s) and the ratio between remnant polarization and maximum polarization (P_r/P_s) versus the applied electric field for the polymers. —◆—: P_s of polymer **II**; —◇—: P_r/P_s of polymer **II**; —■—: P_s of polymer **II′**; —□—: P_r/P_s of polymer **II′**; —▲—: P_s of polymer **III**; —△—: P_r/P_s of polymer **III**.

As shown in Figure 7, the stored energy density of the polymer films as a function of the applied electric field were measured using the Sawyer-Tower circuit under unipolar electric fields of 10 Hz.[5,29] The stretched polymer film **II′** exhibits the highest energy density of more than 10 J/cm^3 under 400 MV/m. As the energy density is proportional to the square of the electric field, this high energy density is achieved through great improvement in the film quality and the breakdown field via mechanical stretching. The electromechanical breakdown has been identified as the primary mechanism of electric failure for these ferroelectric polymers at room temperature.[19] Therefore, higher molecular weight polymer **III** possesses a much higher breakdown strength than polymer **I** with a lower molecular weight, which consequently gives rise to a higher energy density in polymer **III**.

Conclusions

The ferroelectric P(VDF-TrFE-CTFE) terpolymers containing 78.8 mol% VDF, 7.2 mol% TrFE and 14.0 mol% CTFE with different molecular weights have been prepared and characterized. It was found that the crystallinity, thermal properties, polarization hysteresis and relaxation process can be greatly modulated by the molecular weight of the polymers. High molecular weight and broad molecular weight distribution can enhance the inter- and intra-chain entanglement, leading to the decreases of crystallinity and dielectric permittivity. High molecular weight polymer usually leads to an increased breakdown strength, which in turn results in an enhanced stored energy density. By uniaxially stretching of the polymer film, the crystallinity and crystal size increase; this is responsible for the increased maximum applied electric field and higher energy density.

Acknowledgements: This work is supported by the National Science Foundation and the Office of Naval Research.

[1] J. M. Herbert, A. M. Glass, T. T. Wang, In: "*The Application of Ferroelectric Polymers*", Chapman & Hall, New York **1988**.

[2] R. Naber, C. Tanase, P. Blom, G. H. Gelinck, A. W. Marsman, F. J. Touwslager, S. Setayesh, D. M. de Leeuw, *Nat. Mater.* **2005**, *4*, 243.

[3] K. Müller, I. Paloumpa, K. Henkel, D. Schmeisser, *J. Appl. Phys.* **2005**, *98*, 056104.

[4] B. Stadlober, M. Zirkl, M. Beutl, G. Leising, *Appl. Phys. Lett.* **2005**, *86*, 242902.

[5] B. Chu, X. Zhou, K. Ren, B. Neese, M. Lin, Q. Wang, F. Bauer, Q. M. Zhang, *Science* **2006**, *313*, 334.

[6] H. S. Nalwa, in: "*Ferroelectric Polymers*", Marcel Dekker, New York **1995**.

[7] A. J. Lovinger, *Science* **1983**, *220*, 1115.

[8] T. Furukawa, *Phase Transitions* **1983**, *18*, 14.

[9] T. Furukawa, *Adv. Colloid Interface Sci.* **1997**, *71–72*, 183.

[10] G. T. Davis, T. Furukawa, A. J. Lovinger, M. G. Broadhurst, *Macromolecules* **1982**, *15*, 329.

[11] Y. Higashihata, J. Sako, T. Yagi, *Ferroelectrics* **1981**, *32*, 85.

[12] Y. Tajitsu, A. Chiba, T. Furukawa, M. Date, E. Fukada, *Appl. Phys. Lett.* **1980**, *36*, 286.

[13] T. Yagi, M. Tatamoto, J. Sako, *Polym. J.* **1980**, *12*, 209.

[14] T. Yamada, T. Ueda, T. Kitayama, *J. Appl. Phys.* **1981**, *52*, 948.

[15] H. Xu, Z. Cheng, D. Olson, T. Mai, Q. M. Zhang, G. Kavarnos, *Appl. Phys. Lett.* **2001**, *78*, 2360.

[16] F. Xia, Z. Cheng, H. Xu, H. Li, Q. M. Zhang, G. J. Kavarnos, R. Y. Ting, G. Abdel-Sadek, K. D. Belfield, *Adv. Mater.* **2002**, *14*, 1574.

[17] H. Xu, D. Shen, Q. M. Zhang, *Polymer* **2007**, *48*, 2124.

[18] Q. M. Zhang, V. Bharti, X. Zhao, *Science* **1998**, *280*, 2102.

[19] J. Claude, Y. Y. Lu, Q. Wang, *Appl. Phys. Lett.* **2007**, *91*, 212904.

[20] J. Claude, Y. Y. Lu, Q. Wang, *Chem. Mater.* **2008**, *20*, 2078.

[21] Y. Y. Lu, J. Claude, L. E. Norena-Franco, Q. Wang, *J. Phys. Chem. B.* **2008**, *112*, 10411.

[22] Y. Y. Lu, J. Claude, B. Neese, Q. M. Zhang, Q. Wang, *J. Am. Chem. Soc.* **2006**, *128*, 8120.

[23] Y. Y. Lu, J. Claude, Q. M. Zhang, Q. Wang, *Macromolecules*, **2006**, *39*, 6962.

[24] S. H. Zhang, R. J. Klein, K. L. Ren, B. J. Chu, X. Zhang, J. Runt, *J. Mater. Sci.* **2006**, *41*, 271.

[25] S. H. Zhang, B. B. Neese, K. L. Ren, B. J. Chu, Q. M. Zhang, *J. Appl. Phys.* **2006**, *100*, 044113.

[26] J. D. Ferry, in: "*Viscoelastic Properties of Polymers*", Wiley, New York **1980**.

[27] R. G. Kepler, Chapter 3 in: "*Ferroelectric Polymers*", H. S. Nalwa, Ed., Marcel Dekker, Inc., NY **1995**.

[28] H. Su, A. Strachan, W. Goddard, III, *Phys. Rev.* **2004**, *B70*, 064101.

[29] J. K. Sinha, *J. Sci. Instrum.* **1965**, *42*, 696.